

Supplementary Material

Hamdan et al.

Interactive Enhancer Hubs (iHUBs) Mediate Transcriptional Reprogramming and Adaptive Resistance in Pancreatic Cancer

Supplementary Figure Legends

Supplementary Materials and Methods

Rigor and Reproducibility

Table S1, Gene signature in resistance [attached]

Table S2, De-identified patient information [chemotherapy response]

Accession Numbers for Next-generation Datasets

Table S3-S5

Supplementary References

Supplementary Figures S1-S10

Supplementary Figure Legends

Fig.S1 (a-b) Relative confluence plots for treatment of Par and PacR with increasing concentrations of paclitaxel. The confluence is calculated by live cell imaging and represents an experiment where multiple increasing concentrations of paclitaxel were used and readouts are taken every 24 hours for a total of 7 days. Treatment with paclitaxel is renewed every 48 hours. Relative confluence is normalized to 0nM. **(c)** Delta in tumor volume plot showing difference in xenograft volume after different numbers of days of paclitaxel treatment. **(d-e)** box plots showing end weight and volume for xenograft-derived tumors from Par and PacR cells with vehicle and paclitaxel treatment. **(f)** MA plot output of DESeq2 showing significantly regulated genes in PacR cells compared to Par. Each red dot represents a gene that is significantly differentially regulated when comparing PacR to Par. **(g)** GSEA plots comparing the enrichment of activated genes in PacR in PDXBo103 treated vs vehicle (left plot) and PDXGo13 treated vs vehicle (right plot). **(h)** Plot showing normalized counts for the leading genes in the GSEA analysis comparing the treated vs vehicle PDXs.

Fig.S2 (a) Venn diagram showing the overlap between significantly upregulated genes in PacR and significantly upregulated genes in GemR. 7.5% of PacR UP genes are shared with GemR (94 genes). **(b)** GSEA plot for 241 genes that are UP in PacR and treated PDXs showing no enrichment in GemR cells compared to Par, NES -1.47 meaning significant downregulation. **(c)** Heatmap showing H3K4me3 intensity at H3K4me3 peaks in Par and PacR. **(d)** Heatmap and boxplot for input intensity in Par and PacR at the amplified regions in PacR. They show a significant increase of input signals at amplified regions. **(e)** Copy ratio plot showing the amplified regions in PacR compared to Par. **(f)** Pie chart showing that 244 out of 623 significantly downregulated genes in PacR cells interacting with enhancer regions that significantly lose

H3K27ac enrichment [H3K27ac enrichment for these enhancers is shown in the heatmap and boxplot].

Fig.S3 (a) Differential binding plot showing significant regions with gained enrichment of BRD4 in PacR compared to Par. Pink dots represent regions with significant differential enrichment of H3K27ac in PacR compared to Par. **(b)** PCA plot for BRD4 ChIP seq showing distinct separation of BRD4 ChIP samples for Par and PacR. **(c)** Western blot for BRD4 in PacR and Par with HSC70 as a loading control. Ns: Non-specific. **(d)** Box plot showing the stratification of enhancer regions based on their BRD4 intensity into four groups: low, medium, high, and very high. The difference in intensity between each group is significant. **(e)** Gene set enrichment analysis for iHUB interacting genes showing significant upregulation in PacR compared to Par. **(f)** Gene set enrichment analysis for iHUB interacting genes showing no significant enrichment in GemR compared to Par. FDR= 0.55. This shows that the iHUB mechanism is specific to PacR. **(g)** Profile plot showing the intensity of H4K5ac enrichment at iHUB regions (-/+ 2kb) comparing Par (gray) and PacR (pink). Line shows mean RPKM with the light shading representing standard error. Box plot shows significant upregulation for intensity shown in the plot profile. **(h)** Heatmap for H3K4me3 at TSS of genes interacting with iHUBs. **(i)** Box plot showing ChRO-seq signal at iHUBs with more significant signal at PacR compared to Par. **(j)** Venn diagram showing the overlap between super enhancers and iHUBs [point of view of SE].

Fig.S4 (a) Table showing TCGA patients and their predicted IC50 for paclitaxel. **(b)** PCA plot for RNA-seq from the TCGA patients in A showing distinct separation between responsive and nonresponsive patients. **(c)** Correlation plot for base expression and Log2Fold change of genes that are enriched in less responsive patients compared to more responsive. **(d)** Intensity of BRD4 in RPKM at LIF and GPX4 iHUBs in Par and PacR. **(e-g)** BRD4/ H3K27ac occupancy profiles of at non-iHUB active enhancers in PacR with comparable interaction frequencies in Par and PacR.

Fig.S5 (a) Box plot for number of interactions at active enhancers in PacR showing no significant differences between Par and PacR. The two sets of enhancers are identified by the random tool of bedtools with each set including comparable size enhancers. **(b-c)** Coordinates showing the size and placement of cutting regions for LIF iHUBs (b) and GPX4 iHUBs (c). **(d-e)** PCR for validation of iHUB deletion in clonal cell lines showing successful deletion of iHUB regions. **(f)** Western blot showing decreased expression of LIF in the PacR cell line with deleted LIF iHUBs. **(g)** Column bar graphs for qPCR showing gene expression of *SBNO2*, *CBARP*, *STK11* [genes of the vicinity of GPX4] and *CASTOR1*, *TBC1D10A* [genes in the vicinity of LIF] in PacR cell lines with deletion iHUB deletion. No downregulation is observed for any of these genes upon the iHUB deletion.

Fig.S6 (a) Quantification of crystal violet assay in Fig.3D showing relevant confluence (RC) normalized to 0nM showing significant partial sensitization to paclitaxel in PacR cell lines with iHUB deletion. **(b)** Column bar graph for relevant confluence normalized to 0nM in PacR cells treated with 250nM of EC330, the LIF-LIR signaling inhibitor. Cells are co-treated with paclitaxel and EC330 for 5 days [treatment every 48 hours]. **(c)** Column bar graph for relevant confluence normalized to 0nM in PacR cells with knockdown of GPX4 (left) Knockdown cells are treated (for 48 hours) after 24 hours of knockdown. On the right, column bar graph showing gene expression data by qPCR for GPX4 after knockdown for 48 hours [sister plates of the proliferation assay shown on left). **(d-e)** proliferation plots of PacR and Capan-1 cells when treated with 100nM of ML-162 (GPX4 inhibitor) combined with increased concentrations of paclitaxel.

Fig.S7 (a) Heatmap and boxplot showing intensity of JunD binding at iHUBs (+/- 5kb) in Par and PacR. **(b)** Occupancy profiles for JunD in PacR (Pink) and Par (Gray) for TRIM62 iHUB and B3GAT3 iHUB. iHUB is marked by the red arrow. **(c)** Column bar graph for qPCR data showing the significant decrease in 24 hours of JunD knockdown. **(d)** Column bar graph for qPCR data

showing gene expression of the iHUB eRNA [eTRIM62, eC2CD2L, ePTGS2] upon knockdown of JunD in Par and PacR cells.

Fig.S8 (a-c) Interactions defined by H3K4me3 HiChIP where each arc represent an interaction between the two coordinates in 3D. Data is shown in duplicates with nontargeting shown in black and siJunD shown in green.

Fig.S9 (a) Column bar graph for qPCR showing gene expression for eLIF and eGPX4 in Par and PacR. **(b)** qPCR for LIF and eLIF upon treatment with different concentrations of Enitociclib in Par cells. **(c)** Proliferation plots of PacR in MIAPaCa-2 cells when treated with 25nM Enitociclib combined with increased concentrations of paclitaxel. **(d)** plot showing interaction frequency detected by 4C-seq at the GPX4 iHUB as a focal viewpoint. Increase in the counts signifies more interaction with the viewpoint. Interaction frequency is increased in PacR compared to Par and gained interactions are significantly decreased upon treatment with Enitociclib (100nM for 4 h).

Fig.S10 (a) Column bar graph for qPCR data showing gene expression of the iHUB eRNA [eLIF, eGPX4, eLMTK2, eC2CD2L, ePTGS2, eTRIM62,] in PDXs treated with Enitociclib (Fig.6B). **(b)** Semiquantitative IHC intensity scores corresponding to Fig.7A .

Supplementary Materials and Methods

Cell Culture

L3.6pl cells were maintained in phenol red-free minimum essential media (MEM; Thermo Fischer scientific). MIAPaCa-2 cells were maintained in Dulbecco's Modified Eagle Medium (DMEM; Corning) and CAPAN-1 cells were maintained in RPMI 1640 Medium (Corning). Media was supplemented with 10% FBS (Corning), 1% Penicillin/streptomycin (Thermo Fischer scientific). Cells were split upon 80% confluence. Knockdown was performed using Lipofectamine RNAiMAX (Thermofisher) as recommended by the manufacturer and as previously described¹. Smart pools were obtained from the human siGenome (horizon discovery) .

Proliferation Assays

For crystal violet assays [Fig1B, Fig3D, FigS6A] 5000 cells were seeded in each well of a 24-well plate (CELLSTAR) and left to grow overnight. Cells were treated with different concentrations in 0.01% DMSO for 5 days while treatment was replenished every 48 hours. For GPX4 depletion, knockdown was performed while seeding 50,000 PacR cells (reverse transfection). On the following day, cells were treated with different concentrations of paclitaxel for 48 hours. At endpoint, cells were fixed with methanol for 10 minutes and stained with Crystal Violet (1% In 20% Ethanol; Cardinal Healthcare). For quantification in crystal violet assays, stained cells were solubilized in 100mM sodium citrate in 50% ethanol solution. Upon complete solubilization after agitation for 20 minutes, absorbance was measured at 550nm by a plate reader (SPECTRA max PLUS; Molecular Devices). For live cell imaging shown in Fig.S1A-B), 1000 cells were seeded in each well of a 96-well plate and confluence measured every day using Celigo Imaging Cell cytometer (Nexелеcom Bioscience). For proliferation assay in Fig.S6b, confluence was evaluated by live cell imaging IncuCyte (Essen Bioscience). IC50 was calculated from dose-response curves (three parameters) using GraphPad Prism 9.

Chemical agents used in this manuscript include:

Agent	Item No.	Source
Paclitaxel	10461	Cayman Chemical
Trametinib (GSK1120212)	S2673-10MG	SELLECK CHEMICALS LLC
ML-162	20455	Cayman Chemical
Enitociclib (BAY1251152)	HY-103019-50mg	MedChem Express
EC330	S0472-5MG	SELLECK CHEMICALS LLC

Transcriptional Profiling

RNA was extracted using miRNeasy kit (Qiagen) following manufacturer's instructions. Complementary DNA was generated qScript cDNA synthesis kit (Quantbio). Quantitative real time PCR (qPCR) was performed using SsoAdvanced Universal SYBR Green Supermix (BioRAD as instructed. The PCR program run comprised of 2 minutes of initial denaturation at 95°C followed by 40 cycles of 10 seconds at 95°C and 30 seconds at 60 °C. Gene expression changes were evaluated using the starting quantity method and plotted on GraphPad Prism 9. Relative mRNA was normalized to RPLP0 in all cell line experiments. For evaluating eRNA in PDXs, relative eRNA expression was normalized to RPLP0 in addition to the lncRNA MALAT1. Primers used in this study included:

Gene	Forward sequence (5'-3')	Reverse sequence (5'-3')
GPX4	GAGGAGCCCCCTGGTGATAGA	GATTTTCGGGTCTGCCCA
JunD	CCCCTTCGGTTCTTTTCGACC	CGGGCGAACCAAGGATTA CA
LIF	TCCCGGCTAAATATAGCTGTTTCTG	CCGGCAGTTTTTCAGAGTTCA
eLIF	GAATTCCTCCCAAGACCAGCGA	GATGGGGAAGGAAGGAGGGA
eGPX4	TCCAGGAGGGGGAACG	CACTGGGCTGACCACTGC
RPLP0	GATTGGCTACCCAAGTGTG	CAGGGGCAGCAGCCACAAA
HPRT	GCTGACCTGCTGGATTACAT	CCCTGTTGACTGGTCATTACA
SBNO2	AGGAAGAAGCAAGTGGGCATC	TGCCTGCGCTTCACGTC
CBARP	AAGGCACCTCGTTGGATGC	ACCTTGAAATAGGGGCTGGC
STK11	GTGCCCGGTGGCGAG	TCTTTATGACACGGCCAGC
CASTOR1	AGCTGCACATCCTAGAACC	CTGAAGAACTTGCACCGGC
TBC1D10A	CGCGCTGGAGGAAGTACC	ACATGTCCAGCTCGTCAAAC
eTRIM62	TGTTCTGTGAAGAAGAGACAGGG	CCAGCACCACCCTTACATAC
eC2CD2L	GTAGACCGGTGAAGCACGAC	AGCAGTTACACTGCGGGC
ePTGS2	TGTTGAATGCTACTGAGAAGCCAA	TCCCTCTACTGTGCTGAATTGAC
eLMTK2	AGTCCCCGTTCTGGTCCAAT	CATGCAGCGTCATCCTCTGT

Western Blot

Western Blots were performed as reported previously in Kutschat Hamdan et al.². Antibodies used in this manuscript include BRD4 (ab12887; abcam), LIF (NBP2-27406SS, FISHER HEALTHCARE) and HSC70 (SC-7298; Santa Cruz Biotechnology).

RNA-seq

The integrity of RNA was validated by gel electrophoresis and 500ng were used to make the libraries in triplicates for each condition. Libraries for cells were made using the TruSeq RNA Library Prep Kit V2 (Illumina) according to the manufacturer's instructions. Briefly, Oligo-dT beads were used to capture poly-A tailed-mRNA followed by first strand cDNA synthesis by Superscript II reverse transcriptase (Thermo Fischer). Second strand synthesis was followed by end repair, 3' adenylation, adapter ligation and library amplification. Agencourt AMPure XP (Beckman Coulter) was used for size selection during the library synthesis. The quality of the resulting DNA was measured with high sensitivity DNA kit (Agilent) on the Agilent Bioanalyzer 2100. Samples were sequenced (single-end 50 bp) on a HiSeq4000 (Illumina) in the Transcriptome and Genome Analysis Laboratory (TAL) at the University Medical Center Göttingen. Libraries for PDXs were generated similarly using the TruSeq stranded mRNA kit (Illumina) according to instructions. sparQ PureMag Beads (Quantabio) was used for size selection. RNA from-seq from PDX was done in single replicates for each condition. Non targeting PacR and siJunD knockdown were done in duplicates. RNA-seq from Par and PacR were done in triplicates. Samples from Par and Pacr were sequenced (single end 50bp)on HiSeq4000(Illumina) in the Transcriptome and Genome Analysis Laboratory (TAL) at the University Medical Center Göttingen. RNA from PDX were sequenced (paired end 50 bp) on HiSeq4000 (Illumina) in the Genome Analysis Core at the Mayo Clinic. Samples from PacR (NT5 and JunD) were sequenced (paired end 50bp) on NextSeq 2000 (P2) in the Genome Analysis Core at the Mayo Clinic

Chromatin immunoprecipitation (ChIP-seq)

Chromatin immunoprecipitation was performed as described previously¹. Briefly, cells were crosslinked using 1% formaldehyde for 20 minutes and nuclear pellets were sonicated in sonication buffer (150mM NaCl, 20 mM EDTA, 50 mM Tris-HCl (pH 8), 1% v/v NP-40, 0.5% v/v sodium deoxycholate, 20 mM NaF, 0.1% SDS) for 30 cycles using a Bioruptor Pico (Diagenode) and a cycle setting of 30 s on/off. Samples were precleared by 50% slurry of Sepharose 4B (GE Healthcare) and incubated with antibody overnight. Antibodies included H3K27ac (1µg; C15410196, Diagenode), H3K4me3 (1µg; C15410003, Diagenode), H4K5ac (2µg; C15410025, Diagenode), Pol II D8L4Y (5µl; 14958, Cell Signaling), MED1 (2µg; A300-793A, FISHER HEALTHCARE), JunD (5ul; 61403, ACTIVE MOTIF), and control rabbit IgG (1µg; C15410206, Diagenode). Protein A-sepharose beads were added to samples and incubated for 2 hours, then washed, de-crosslinked, and DNA was extracted. Samples were performed in duplicates for each condition (except Pol II). Libraries were prepared using the MicroPlex Library Preparation Kit v2 (Diagenode) according to manufacturer's protocol. DNA integrity was measured with high sensitivity DNA kit (Agilent) on the Agilent Bioanalyzer 2100. ChIP for H3K27ac, BRD4, H4K5ac, JunD and inputs were done in duplicates, and ChIP for H3K4me3, MED1, and Pol II were done in singular replicates. H3K27ac and BRD4 samples were sequenced (single-end 50 bp) on a HiSeq4000 (Illumina) in the Transcriptome and Genome Analysis Laboratory (TAL) at the University Medical Center Göttingen. H3K4me3 and PolII samples were sequenced (paired end 50 bp) on a HiSeq4000 (Illumina) in the Genome Analysis Core at the Mayo Clinic. H4K5ac, MED1 and JunD were sequenced (paired end 50 bp) on NextSeq2000 (P2, Illumina) in the Genome Analysis Core at the Mayo Clinic.

H3K4me3 HiChIP

HiChIP was performed based on Gryder et al.^{3,4} with minor modifications as described previously⁵. Briefly, cells were washed with PBS and trypsinized. As a spike-in control, 1.25 millions of mouse

NIH/3T3 cells were added to 5 million cells of Par and PacR cells in duplicates. Cells were fixed for 10 minutes with 1% Formaldehyde and suspended in ice-cold Hi-C Lysis Buffer (10mM Tris-HCL pH 7.5, 10mM NaCl, 0.2% NP-40 in water). Nuclear DNA was digested for 2 hours at 700rpm with 200 unites each of Mbol, DpnII, and Hinf1 (NEB).

This was followed by biotin incorporation for 1 hour at 300 rpm using Biotin-14-dATP (Thermo Fisher) and DNA Polymerase I Large (Klenow) Fragment. DNA was ligated at 23°C for 4 hours at 300rpm using T4 DNA ligase (NEB). Subsequently, samples were sonicated using the Bioruptor Pico machine (Diagenode) in the same sonication as ChIP-seq for 10 cycles. Same ChIP protocol steps were followed until DNA extraction. Then, Streptavidin-C1 beads (Thermo Fisher) were used to capture biotinylated DNA followed by library preparation using the MicroPlex Library Preparation Kit v2 (Diagenode) Samples for Par and PacR were done in singular replicates. Samples from NT5 PacR and siJunD PacR were done in duplicates. Par and PacR samples were sequenced 50 PE on HiSeq4000 (Illumina). PacR (NT5 and siJunD) were sequenced 50 PE on NextSeq 2000 (P2, Illumina). All HiChIP sequencing was performed in the Genome Analysis Core at the Mayo Clinic.

leChRO-seq

LeChRO-seq libraries were prepared following the protocol from Chu et al⁶. Briefly, cells were collected and washed in PBS once, while 30mg of PDX were homogenized using Biomasher II (VWR). Chromatin was harvested by incubating the samples in NUN buffer (20mM HEPES pH 7.5, 7.5mM MgCl₂, 0.2mM EDTA, 0.3M NaCl, 1M Urea, 1% NP-40, 1mM DTT, RNase Cocktail and protease inhibitors (cOmplete mini EDTA-free tabs; Roche Biochem)) for 30min at 4 °C, 1,500 rpm, washing twice with 50mM Tris-HCl with 0.04 units/μl of SUPERase RNase inhibitor (AM 2694; Life technologies) and resuspending in chromatin storage buffer (50mM Tris-HCl, 25% Glycerol, 5mM MgAc₂, 0.1mM EDTA, 200mM DTT, 0.04 units/μl of SUPERase RNase inhibitor. Subsequently, chromatin was sonicated using a Bioruptor Pico (Diagenode). For the run-on

reaction 50 μ l of chromatin extract were mixed with 50 μ l of 2x Biotin-11 run on reaction mix (10mM Tris-HCl pH 8, 5mM MgCl₂, 1mM DTT, 300mM KCl, 400 μ M ATP (N0450S;NEB), 0.8 μ M UTP (N0450S;NEB), 400 μ M GTP (N0450S; NEB), 400 μ M CTP (N0450S;NEB), 40 μ M Biotin - 11-UTP (NEL543001EA;Perkin Elmer), 100ng yeast tRNA (80054-306; VWR), 0.8 units/ μ l SUPERase RNase inhibitor and 1% Sarkosyl (AC612075000; Fisher Scientific) and incubated at 37 °C 700 rpm for 5 min. The reaction was stopped using 500 μ l of TRIzol LS (10296-010; Life technologies) and the RNA pelleted using GlycoBlue (AM9515; Ambion). Nascent, biotinylated RNA was captured using hydrophilic streptavidin magnetic beads (S1421S; NEB) and washed twice with high salt (50mM Tris-HCl pH 7.4, 2M NaCl, 0.5% Triton X-100, 0.004 units/ μ l of SUPERase RNase inhibitor, twice with binding buffer (10mM Tris-HCl pH 7.4, 300mM NaCl, 0.1% Triton X-100, 0.004 units/ μ l of SUPERase RNase inhibitor and once with low salt buffer (5mM Tris-HCl pH 7.4, 0.1% Triton X-110, 0.004 units/ μ l of SUPERase RNase inhibitor. TRIzol (15596-026; Life technologies) was used to extract RNA from the beads, which was precipitated using GlycoBlue (AM9515; Invitrogen). 3' RNA adaptors were ligated using T4 RNA ligase (NEB), the RNA captured using hydrophilic streptavidin magnetic beads (NEB), the beads washed, and the RNA extracted as described above. Following, the 5' end of the extracted RNA was de-capped using RppH (NEB,) and phosphorylated using PNK (NEB). RNA was extracted using TRIzol (15596-026; Life technologies) and 5' RNA adaptors ligated using T4 RNA ligase (NEB). A third biotin enrichment was performed as described above prior to reverse transcription using Superscript III (12574026; Invitrogen). Phusion High Fidelity DNA Polymerase (F530S; ThermoFisher Scientific) was used to PCR amplify the library, which was then submitted to a post-PCR cleanup using AMPure XP beads (Beckman Coulter). Finally, DNA concentration was measured using Qubit (ThermoFisher Scientific) and library quality was assessed using the high sensitivity DNA kit (Agilent) on the Agilent Bioanalyzer 2100. leChRO-seq from Par is available in duplicates and singular replicate in PacR. Samples were sequenced (paired-end 50 bp) on HiSeq4000 (Illumina) in the Genome Analysis Core at the Mayo Clinic.

ATAC-seq

ATAC-seq (Omni-ATAC-seq) was performed as described in Corces et al. ⁷. Briefly 50,000 cells were counted and resuspended in freshly prepared ATAC resuspension buffer A (10mM Tris HCL pH 7.4, 10mM NaCl, 3mM MgCl₂ in water). Sample was incubated at a rotating wheel at 4°C for 15 minutes followed by adding 1 ml of ATAC resuspension buffer B (0.1% NP40, 0.1% Tween-20, and 0.01% Digitonin in ATAC resuspension buffer A). Nuclear DNA was tagmented using Tn5 Transposase at 37°C for 30 min at 1000 RPM (Illumina Tegment DNA Enzyme and Buffer Small Kit; 20034197; Illumina). DNA was extracted using the MinElute PCR Purification kit (Qiagen). Then DNA was amplified for 5 cycles and extracted followed by quality validation using the Bioanalyzer 2100 (Agilent). ATAC seq was performed in duplicates. Samples were sequenced (paired end 50 bp) on HiSeq4000 (Illumina) in the Genome Analysis Core at the Mayo Clinic.

4C-seq at iHUBs

4C-seq at the iHUBs of *LIF* and *GPX4* were performed following the method protocol described by Krijger et al.⁸ Briefly, 8 million cells were treated for 4 hours with vehicle or Enitociclib. Then cells were trypsinized and crosslinked using 2% Formaldehyde for 10 minutes. Cells were lysed in freshly prepared cold cell lysis buffer (50mM Tris-HCL pH 7.5, 0.5% NP-40, 1% Triton-X100, 150mM NaCl, 5mM EDTA in water) supplemented with protease inhibitors (cOmplete mini EDTA-free tabs; Roche Biochem). Then samples were lysed at 37°C in restriction buffer with SDS to a final concentration of 0.3% followed by an hour in 2.5% Triton-X. Subsequently, samples were digested (**first digestion**) using 100 U of **Csp6I (CviQI)** (NEB) at 37 °C while shaking at 750 rpm then adding another 100 U and leaving at 37 °C overnight. Then samples were ligated using T4 ligase (Roche) in total 7 ml reaction volume at 16 °C overnight. DNA was then extracted, and DNA digested (second digestion) using 50 U **NlaIII** (NEB) at 37 °C at 500 rpm overnight. Then DNA was ligated using 50 U T4 ligase in ligation buffer with a DNA concentration of 5ng/ul. Upon DNA extraction, libraries were prepared by enriching for viewpoint enrichment using Expand Long

Template Polymerase mix (Roche) in a PCR program including 2 min of 94 °C and 16 cycles of (94 °C for 10s, 60°C for 10s for 1 min, 68°C for 3 min) and 5 minutes of extension at 68°C. Primers used at this step are:

Primer	sequence (5'-3')
LIF Reading primer	TACACGACGCTCTTCCGATCTCTAGACTTC CTTCCCCATCCCCTCT
LIF Non-reading primer	ACTGGAGTTCAGACGTGTGCTCTTCCGAT CTAGTTCAGGGACCTCCCATCTCACC
GPX4 Reading primer	TACACGACGCTCTTCCGATCTGCTGGACA GGTGACATCAGCACTGG
GPX4 Non-reading primer	ACTGGAGTTCAGACGTGTGCTCTTCCGAT CTTCTGCGGAGTCTGACCACCTCCTCTG

Adapter ligation was performed exactly as explained in Krijger et al. and DNA extracted using the MinElute PCR Purification kit (Qiagen). Quality validation was performed using the Bioanalyzer 2100 (Agilent). 4C seq at LIF iHUBs were done in duplicates, GPX4 iHUBS were done in singular replicates. Samples were sequenced (paired end 100 bp) on HiSeq4000 (Illumina) in the Genome Analysis Core at the Mayo Clinic.

Cas9 deletion of iHUBs

Cas9 expressing Par and PacR cells were generated exactly as described in Kutschat Hamdan et al.² using the lentiCas9-Blast (Plasmid no.52962; addgene). gRNA were designed to flank the iHUB (left and right) using CRISPOR⁹. Synthetic gRNAs (SC1969; GenScript) were transfected into cells using Lipofectamine RNAiMAX (Invitrogen) according to manufacturer's protocol. After 24 hours, clonal cells were seeded for proliferation assay and after 48 hours, RNA was extracted from cells. Synthetic gRNA used in this paper include:

gRNA	sequence (5'-3')
gRNA LIF iHUB 1	TCACAGTCAGGCATTCTGTG
gRNA LIF iHUB 2	TCAGGTGGGCCTAGGAAGGA
gRNA GPX4 iHUB 1	AGATGAATTTCTCAGTGCCA
gRNA GPX4 iHUB 2	ACGGGGACTTGGGGAAAAC

To validate the knockout, we used GoTaq DNA Polymerase (Promega) according to the manual instructions. PCR cycles included 2 min of 95 °C and 30 cycles of (94 °C for 30s, 60°C for 30s, 72°C for 1 min) and 5 minutes of extension at 72°C. Primers used at this step are:

Primers	Sequence (5'-3')
LIF_iHUB_Cas_F1	CCTGATCTGAGGACAGCAGC
LIF_iHUB_Cas_R1	TGGTGGCATCACACTCTCAC
LIF_iHUB_Cas_F2	GCCCCATGTGAGAAGGAAGG
LIF_iHUB_Cas_R2	CACTGGGGTGAGAACAGTGG
GPX4_iHUB_Cas_F1	ACAGAAAATGCGAGGGAGGG
GPX4_iHUB_Cas_R1	TTGTGCCCTGTAGATGCTGG
GPX4_iHUB_Cas_F2	AAGTAGGGCACCAGAGGAGAT

leChRO-seq Bioinformatic Analysis

The leChRO-seq data was analyzed as previously described⁶. In brief, reads were first preprocessed to remove adapters and low-quality sequence. Following that, UMI (unique molecular identifiers) were used to remove PCR duplicates. Subsequently, the preprocessed reads were then mapped to hg19 reference genome using BWA 0.7.12-r1039¹⁰. Then the 5' ends of mapped reads, which indicated the exact position of polymerases, were exploited to generate bedGraph and BigWig files for each DNA strand. Stranded bigwigs were used to assess intensity and plot heatmaps (plotHeatmap) and profiles (plotProfile) using computeMatrix in deepTools/3.3.2¹¹.

RNA-seq Bioinformatic Analysis

Bam files were generated by mapping raw reads by STAR/2.7.3a¹². Features were counted using htseq/0.9.1¹³. Differential gene expression analysis was performed by DESeq2¹⁴. Gene set enrichment analysis (GSEA)¹⁵ was performed with default settings using normalized counts from DESeq2 for expressed genes. GSEA 4.2.3 for samples including 1/2 replicates were performed with Difference of classes and abs gene list sorting mode. Upregulated genes were identified as >0.7 log2 Fold change and FDR<0.05. For RNA-seq taken from TCGA through CancerRxTissue,

we picked samples on the two opposite ends of paclitaxel IC50 (sensitive vs resistant) and focused on samples that are transcriptionally distinct in principal component analysis.

ATAC-seq Bioinformatic Analysis

Adapters were trimmed from fastq files using cutadapt/2.8¹⁶. This was followed by mapping to the hg19 genome using Bowtie2¹⁷. Big fragment were filtered using AlignmentSieve in deepTools/3.3.2¹¹. Bigwigs were generated with bamCoverage and peaks called with MACS2 without inputs¹⁸.

ChIP-seq Bioinformatic Analysis

Mapping of reads was performed to the reference genome assembly (hg19) by BOWTIE2/2.2.5¹⁷. Bigwig files were generated by ignoring duplicates and extending to 200 bp for ChIP samples that are single end using bamCoverage. Localization profiles were viewed using the Integrative Genomics Viewer (IGV 2.8.0)¹⁹. MACS2¹⁸ was used to call the significant peaks without building the shifting model and with --broad-cutoff 0.05 for BRD4 and H3K27ac and input files from respective cells as background. The Bioconductor R package Diffbind 2.14.0²⁰ was run on R version 3.6.0 according to the instruction manual to define regions were differentially enriched by H3K27ac or BRD4. ChIP Occupancy was evaluated by the computeMatrix tool and the average profiles and heatmaps were generated based on computeMatrix values with the ploheatmap tool. Boxplot were plotted using GraphPad Prism 9. The ROSE algorithm was used to identify super enhancers from stitched regions of H3K27ac regions and BRD4 signal with the default settings with ignoring regions that are 2500 bp around the TSS^{21,22}. Motif analysis was performed using the findMotifs.pl command in HOMER/4.10 with the background as shuffled sequences prepared from the same files with scrambleFasta.pl²³. Distance from TSS were generated by GREAT analysis²⁴. CNV analysis was performed using the CNVkit²⁵ as recommended and previously

described² and supplemented with differential binding analysis for further validation. The chrY was omitted from the genome segmentation as the cell line originates from a female patient.

4C-seq Bioinformatic Analysis

Data was analyzed using 4C-ker²⁶. Fastq files were mapped using bowtie2/2.3.3.1¹⁷ to a reduced hg19 genome flanking the restriction enzymes generated from the bed file output of digest_genome.py of hic_pro/2.10.0²⁷. Counts were created from the SAM file (.bedGraph) using bash provided by 4C-ker. Self-ligated and undigested fragments were removed and 4C-ker object was generated and cis analysis was performed as instructed in the 4C-ker manual.

HiChIP Bioinformatic Analysis

Primary analysis was performed similar to Wang et al.⁵. Briefly, hic_pro/2.10.0²⁷ was used to perform dual mapping and generating valid pairs in hg19 and mm9. We validated that there are consistent ratios of mm9 valid pairs compared to hg19 valid pairs in different condition (Par and PacR) by following analysis protocol in Gryder et al.³ Bedpe files were generated using FitHiChIP²⁸. Bedpe files were visualized in IGV. At regions where interaction arcs are too dense to be distinguishable, iHUB specific interactions (iHUB intersecting with right or left anchor) were filtered and shown. In Par cells, we identified 647510 peak to all interactions. In PacR cells, we identified 739017 peak to all interactions. APA analysis was performed as recommended by Lieberman-Aiden et al.²⁹

Identification of iHUBs

Focusing on ATAC summits in all conditions (168449 regions), we evaluated the intensity of ChRO-seq using computeMatrix at +/- 200bp with singular bin resolution and summed signal. Subsequently, we calculated the ratio of sense and antisense transcription. We filtered for TSS or H3K4me3 and focused on regions that have detectable transcription and have weighted one-

sided transcription (>3 fold). We also included ATAC summits where transcription originate in the opposite direction of a transcribed gene. Then, we filtered for regions that gain BRD4 significantly in resistance irrespective of H3K27ac differential enrichment.

Patient-derived xenograft establishment and treatment (PDX298)

All the planned experiments followed the Guide for the Care and Use of Laboratory Animals of the National Institutes of Health. The animal protocol was approved by the Institutional Animal Care and Use Committee (IACUC) at the Mayo Clinic (#A00003954-18-R21). The animal care facilities and use program meet all federal regulations and guidelines. Mayo Foundation is registered with the USDA (41-R-006) as an animal research facility and maintains an NIH animal assurance statement (A3291-01) with the Office of Laboratory Animal Welfare. The Patient-Derived Xenograft (PDX) resected tumors were obtained from the Mayo Clinic Institutional PDX program in Hepatobiliary and Pancreatic Tumors and aggressive abdominal malignancies collected under Mayo Clinic IRBs (66-06, 354-06, 19-012104).

Experimental units reported in this manuscript is a single animal (i.e., mouse). White albino non-obese diabetic with severe combined immunodeficiency (NOD/SCID) (NOD.CB17-Prkdcscid/NCrCrI) female mice were obtained from Charles River Laboratory (Charles River, USA). The mice's diet was LabDiet PicoLab Rodent Diet 20 (Lab Supply, Fort Worth, Texas). The mice were caged in an Innovative Disposable caging system called Innocage® Mouse Pre-Bedded Corn Cob, housed in the validated Innorack® IVC Mouse 3.5 (Inno Vive, San Diego, California). Five mice are housed per cage in a 12-h light/dark cycle with adequate access to food and water with no fasting.

The cryopreserved basal pancreatic adenosquamous carcinoma PDX tumor was implanted subcutaneously into five mice as described previously³⁰⁻³³. After eight weeks, we humanely euthanized one mouse with a large enough tumor (around 1000 mm³). The tumor was harvested, and one fragment was sent for histology confirmation. The rest of the tumor was passed immediately into the left flank of 20 NOD/SCID 7-weeks-old female mice for each *in vivo* study using the same primary tumor xenograft protocol. Each group included 5 mice (5x4 groups= 20 mice/experiment). The number of mice/group was minimized to 5 mice per group in these two *in vivo* studies to reduce laboratory mice use, considering these as early feasibility/pilot *in vivo* studies (as per ARRIVE Guidelines)³⁴. Mice were included in the specific experiment if they have palpable tumor in the left flank. Mice were excluded if they did not grow tumors or they were less than 40% of the average weight (i.e., 25 gram for female). The data points were collected twice per week. Tumor dimensions were monitored biweekly by manual palpation and digital caliper. When tumors reached a volume of 250 - 500 mm³, the mice were randomized according to the tumor volume into four groups (5 mice/group). The main confounders were used to randomize the mice into groups. All mice were housed in the same floor and under the same conditions. However, each group were living in similarly designed but separate cage for each group. In the first PDX [Experiment 1] *in vivo* study, we divided the mice into the following groups: 1) control without treatment; 2) treated with CDK9i (Enitociclib) (10 mg/kg intravenous injection (IV), once weekly); 3) treated with nab-paclitaxel (30 mg/kg, intraperitoneal injection (IP) biweekly); 4) treated with combination doublet – CDK9i (Enitociclib) (10mg/Kg, IV once weekly), and nab-paclitaxel (30mg/Kg, IP biweekly). One mouse died (from the CDK9i group) before the end of the study. The data

were included till the last day of measurement before death. Statistical analysis was performed on n= 5/4/5/5. In the second PDX [Experiment 2] in vivo study, we had a similar design, but we substituted the CDK9i (Enitociclib) with the MEK inhibitor, Trametinib (0.3 mg/kg, oral by gavage, daily). One mouse died (from the Pac/MEKi group) before the end of the study. The data were included till the last day of measurement before death. Statistical analysis was performed on n= 5/5/5/4. All the drugs were delivered during the light cycle. The treatment studies continued for around three weeks. Tumor volume was the outcome measured and it was calculated as volume = L × W × W (L is the length and W is the width of the tumor). Mouse weight has been measured using a digital scale. Tumor dimensions, volumes, and mouse weights were recorded biweekly and compared between the four groups. The mixed effect model was used to assess the difference in each treatment on the tumor volume at each time point. The statistical program was GraphPad Prism 9. Animals were humanely euthanized on the 24th treatment day by IACUC-trained personnel using carbon dioxide, followed by cervical dislocation. Immediately after, the tumor was harvested, measured, weighed, and pictured.

The corresponding authors (authors who conceptualized and designed the study) were blinded to the group allocation at different stages of the study. The studies were conducted in an independent PDX laboratory. The PDX laboratory scientists and personnel were not blinded to the conduct of the experiments, assessment or data analyses. All the planned experiments followed the Guide for the Care and Use of Laboratory Animals of the National Institutes of Health. The animal protocol was approved by the Institutional Animal Care and Use Committee (IACUC) at the Mayo Clinic (#A00003954-18-R21). The animal care facilities and use program meet all federal

regulations and guidelines. Mayo Foundation is registered with the USDA (41-R-006) as an animal research facility and maintains an NIH animal assurance statement (A3291-01) with the Office of Laboratory Animal Welfare. The resected patient tumors utilized to generate patient-derived xenografts (PDX) were obtained from the Mayo Clinic Institutional PDX program in Hepatobiliary and Pancreatic Tumors and aggressive abdominal malignancies collected under Mayo Clinic IRBs (66-06, 354-06, 19-012104).

Patient-derived xenograft establishment and treatment (PDXGo13/PDXBo103)

PDXGo13 was generated and treated as previously described in Kutschat et al.² PDXGo13 were treated for 3 treatment cycles and PDXBo103 was treated for 6 treatment cycles. Each treatment cycle is defined as 30mg/kg paclitaxel + 100mg/kg gemcitabine together supplemented with 100mg/kg gemcitabine within one week. Protocols used in PDXGo13 generation adhere to the guidelines of the Institutional Animal Care and Use Committee (33.9-42502-04-17/2407). All PDXGo13-related experiments in this study are approved by the UMG IRB (Göttingen, Germany; 70112108). PDX103 was generated similar to PDX13.

Cell-derived xenograft establishment and treatment

The sensitive and resistant cultured cells were trypsinized and neutralized and the cell suspension was transferred to a separate 50 ml falcon tube for each cell type. After cell count, we prepared enough cells (for each cell type we prepared 15×10^6 cells/ 1.5 mL of suspension media and matrigel in 1:1 ratio) for the subcutaneous injection in 15 mice/cell types and kept the cell suspension on ice to prevent matrigel solidification. After proper

analgesia, mice were anesthetized, and minor surgical incisions were on performed on each mouse's left flank. We pipette the cell suspension up and down until a single cell suspension is obtained, and then inject 0.1 mL into the left flank of each mouse using 200ml pipette. We hold the skin incision up by surgical forceps till the implanted cell line suspension with matrigel solidifies after a few seconds, and then the incision was closed using one surgical clip. Each cell line type was implanted into fifteen mice to account for extra mice if needed.

Cell line-derived xenografts tend to grow faster than PDX, so the study started one week after the implantation. The mice were randomized into four groups (5 mice/group) according to the tumor volume: 1) sensitive cell-line derived xenograft control without treatment; 2) sensitive cell-line derived xenograft treated with nab-paclitaxel (30 mg/kg, intraperitoneal injection (IP) biweekly); 3) resistant cell-line derived xenograft control without treatment; 4) resistant cell-line derived xenograft treated with nab-paclitaxel (30 mg/kg, intraperitoneal injection (IP) biweekly). The treatment studies continued for around three weeks. Tumor volume was calculated as $\text{volume} = L \times W \times W$ (L is the length and W is the width of the tumor). Mouse weight has been measured using a digital scale. Tumor dimensions, volumes, and mouse weights were recorded biweekly and compared between the four groups. Animals were humanely euthanized on the 21st treatment day by IACUC-trained personnel using carbon dioxide, followed by cervical dislocation. Immediately after, the tumor was harvested, measured, weighed, and pictured.

Immunohistochemistry (IHC)

Paraffin embedded tissue sections were deparaffinized in 100% Xylene, hydrated in graded ethanol (100%-70%) and then washed with PBS. Antigen retrieval was performed by incubating the slides in 0.01M citrate buffer (pH 6.0) and heated for 45 mins in a steamer. After 20 mins of cool down the sections were washed in water and then PBS. After quenching of endogenous peroxidases with 3% H₂O₂, sections were incubated with Avidin-Biotin block (Vector Laboratories, SP-2002), and then in CAS-blocking buffer (Life Technologies 008120) for 1 hour. Tissues were then incubated with indicated primary antibody (1:500 LIF: LS-B7078-0.05, Lifespan Biosciences, 1:1000 GPX4: HPA058546 sigma Aldrich) overnight at 4°C. Next day, following 3 PBS washes the sections were incubated with respective biotinylated secondary antibodies (Vector Laboratories). After PBS washes, sections were incubated with ABC reagent (Vector Laboratories, PK-7100) for 30 minutes. Sections were developed using the DAB kit (Vector Laboratories, SK-4100) after PBS washes. Following hematoxylin staining (Sigma Aldrich, GHS-232), sections were dehydrated using graded ethanol and Xylene, then mounted using Cytoseal. Scans were taken using ImageXpress Pico (Molecular Devices).

Table S2. Deidentified patient numbers and response information

1	Female	Good Response	Decrease in tumor size
2	Female	Partial Response	Moderate response
3	Male	Good Response	Decrease in tumor size
4	Female	Partial Response	Moderate response
5	Male	Poor Response	No change in tumor size
7	Female	Poor Response	Increase in tumor size
8	Male	Partial Response	Moderate response
9	Male	Good Response	Decrease in tumor size
10	Female	Poor Response	Increase in tumor size

**** Response based on findings after chemotherapy [Gem/Abraxane]**

Accession Numbers for NGS data

**** P.S. All compared experiments were performed at the same time and under the same condition even if in different series**

Table S3. Accession Numbers for RNA and ChRO-seq

No	Application	System	Condition	Rep	Accession Number	Database	Reference
1	RNA seq	L36	Par	1	GSE152121	GEO	Kutschat et al. ²
2	RNA seq	L36	Par	2	GSE152121	GEO	Kutschat et al. ²
3	RNA seq	L36	Par	3	GSE152121	GEO	Kutschat et al. ²
4	RNA seq	L36	GemR	1	GSE152121	GEO	Kutschat et al. ²
5	RNA seq	L36	GemR	2	GSE152121	GEO	Kutschat et al. ²
6	RNA seq	L36	GemR	3	GSE152121	GEO	Kutschat et al. ²
7	RNA seq	PDX13	Veh	1	GSE152121	GEO	Kutschat et al. ²
8	RNA seq	PDX13	Gem Pac	1	GSE152121	GEO	Kutschat et al. ²
9	RNA seq	PDX103	Veh	1	E-MTAB-11739	ArrayExpress	This Study
10	RNA seq	PDX103	Gem Pac	1	E-MTAB-11739	ArrayExpress	This Study
11	RNA seq	L36	PacR	1	E-MTAB-11737	ArrayExpress	This Study
12	RNA seq	L36	PacR	2	E-MTAB-11737	ArrayExpress	This Study
13	RNA seq	L36	PacR	3	E-MTAB-11737	ArrayExpress	This Study
14	RNA seq	L36	Par	1	E-MTAB-12705	ArrayExpress	This Study
11	RNA seq	L36	Par	2	E-MTAB-12705	ArrayExpress	This Study
12	RNA seq	L36	PacR	1	E-MTAB-12705	ArrayExpress	This Study
13	RNA seq	L36	PacR	2	E-MTAB-12705	ArrayExpress	This Study
14	ChRO-seq	L36	Par	1	E-MTAB-11744	ArrayExpress	This Study
15	ChRO-seq	L36	Par	2	E-MTAB-11744	ArrayExpress	This Study
16	ChRO-seq	L36	PacR	1	E-MTAB-11744	ArrayExpress	This Study
17	ChRO-seq	PDX13	Veh	1	E-MTAB-11740	ArrayExpress	This Study
18	ChRO-seq	PDX13	Gem Pac	1	E-MTAB-11740	ArrayExpress	This Study
19	ChRO-seq	PDX103	Veh	1	E-MTAB-11740	ArrayExpress	This Study
20	ChRO-seq	PDX103	Gem Pac	1	E-MTAB-11740	ArrayExpress	This Study

Table S4. Accession Numbers for HiChIP and 4C-Seq

No	Application	System	Cond.	Rep	Accession Number	Database	Reference
1	4CSeq LIF iHUB	Par	veh	1	E-MTAB-11731	ArrayExpress	This Study
2	4CSeq LIF iHUB	Par	veh	2	E-MTAB-11731	ArrayExpress	This Study
3	4CSeq LIF iHUB	PacR	veh	1	E-MTAB-11731	ArrayExpress	This Study
4	4CSeq LIF iHUB	PacR	veh	2	E-MTAB-11731	ArrayExpress	This Study
5	4CSeq LIF iHUB	PacR	VIP	1	E-MTAB-11731	ArrayExpress	This Study
6	4CSeq LIF iHUB	PacR	VIP	2	E-MTAB-11731	ArrayExpress	This Study
7	4CSeq GPX4 iHUB	Par	veh	1	E-MTAB-11731	ArrayExpress	This Study
8	4CSeq GPX4 iHUB	PacR	veh	1	E-MTAB-11731	ArrayExpress	This Study
9	4CSeq GPX4 iHUB	PacR	VIP	1	E-MTAB-11731	ArrayExpress	This Study
10	H3K4me3 HiChIP	Par	**	1	E-MTAB-11732	ArrayExpress	This Study
11	H3K4me3 HiChIP	PacR	**	1	E-MTAB-11732	ArrayExpress	This Study
12	H3K4me3 HiChIP	PacR	NT	1	E-MTAB-12708	ArrayExpress	This Study
13	H3K4me3 HiChIP	PacR	NT	2	E-MTAB-12708	ArrayExpress	This Study
14	H3K4me3 HiChIP	PacR	siJunD	1	E-MTAB-12708	ArrayExpress	This Study
15	H3K4me3 HiChIP	PacR	siJunD	2	E-MTAB-12708	ArrayExpress	This Study

Table S5. Accession Numbers for CHIP and ATAC-seq

No	Application	System	Condition	Rep	Accession Number	Database	Reference
1	ChIP H3K27ac	L36	Par	1	E-MTAB-7034	ArrayExpress	Hamdan et al.
2	ChIP H3K27ac	L36	Par	2	E-MTAB-7034	ArrayExpress	Hamdan et al.
3	ChIP H3K27ac	L36	PacR	1	E-MTAB-11733	ArrayExpress	This Study
4	ChIP H3K27ac	L36	PacR	2	E-MTAB-11733	ArrayExpress	This Study
5	ChIP BRD4	L36	Par	1	E-MTAB-7034	ArrayExpress	Hamdan et al.
6	ChIP BRD4	L36	Par	2	E-MTAB-7034	ArrayExpress	Hamdan et al.
7	ChIP BRD4	L36	PacR	1	E-MTAB-11733	ArrayExpress	This Study
8	ChIP BRD4	L36	PacR	2	E-MTAB-11733	ArrayExpress	This Study
9	ChIP H3K4me3	L36	Par	1	E-MTAB-11733	ArrayExpress	This Study
10	ChIP H3K4me3	L36	PacR	1	E-MTAB-11733	ArrayExpress	This Study
11	ChIP input	L36	Par	1	E-MTAB-7034	ArrayExpress	Hamdan et al.
12	ChIP input	L36	Par	2	E-MTAB-7034	ArrayExpress	Hamdan et al.
13	ChIP input	L36	PacR	1	E-MTAB-11733	ArrayExpress	This Study
14	ChIP input	L36	PacR	2	E-MTAB-11733	ArrayExpress	This Study
15	ChIP Pol II	L36	Par	1	E-MTAB-11733	ArrayExpress	This Study
16	ChIP Pol II	L36	PacR	1	E-MTAB-11733	ArrayExpress	This Study
17	ChIP input	L36	Par	1	E-MTAB-11733	ArrayExpress	This Study
18	ChIP input	L36	Par	2	E-MTAB-11733	ArrayExpress	This Study
19	ChIP JunD	L36	Par	1	E-MTAB-12707	ArrayExpress	This Study
20	ChIP JunD	L36	Par	2	E-MTAB-12707	ArrayExpress	This Study
21	ChIP JunD	L36	PacR	1	E-MTAB-12707	ArrayExpress	This Study
22	ChIP JunD	L36	PacR	2	E-MTAB-12707	ArrayExpress	This Study
22	ChIP MED1	L36	Par NT	1	E-MTAB-12707	ArrayExpress	This Study
23	ChIP MED1	L36	Par siJUND	1	E-MTAB-12707	ArrayExpress	This Study
24	ChIP MED1	L36	PacR NT	1	E-MTAB-12707	ArrayExpress	This Study
25	ChIP MED1	L36	PacR siJUND	1	E-MTAB-12707	ArrayExpress	This Study
26	ChIP H4K5ac	L36	Par NT	1	E-MTAB-12707	ArrayExpress	This Study
27	ChIP H4K5ac	L36	Par NT	2	E-MTAB-12707	ArrayExpress	This Study
28	ChIP H4K5ac	L36	PacR NT	1	E-MTAB-12707	ArrayExpress	This Study
29	ChIP H4K5ac	L36	PacR NT	2	E-MTAB-12707	ArrayExpress	This Study
30	ATAC	L36	Par	1	E-MTAB-11730	ArrayExpress	This Study
31	ATAC	L36	Par	2	E-MTAB-11730	ArrayExpress	This Study
32	ATAC	L36	PacR	1	E-MTAB-11730	ArrayExpress	This Study
33	ATAC	L36	PacR	2	E-MTAB-11730	ArrayExpress	This Study

Rigor and Reproducibility

This study used multiple cutting edge-techniques and bioinformatic analyses to identify a novel subgroup of enhancers. It is important to note that the use of TSS-centric H3K4me3 HiChIP was crucial in the identification of iHUBs, due to the lack of enrichment bias that is exhibited by the highly reprogrammed H3K27ac. We ensured the robustness and reproducibility of our HiChIP data by including spike-in controls from the mouse genome and performing ChIP-independent chromatin conformation assays such as 4C-seq. Any limitations in this study dictated by technical issues were addressed by ensuring that confounding factors are minimized in other systems. For example, resistant cells formed smaller tumor in the xenograft model. While slower proliferation rates protect from chemotoxicity, we ensured that all inhibitors used to sensitize cells have limited effects on cell growth to ensure that the effects are due to molecular mechanisms. To ensure that the effects seen in this study are not cell-specific, we also ensured that any mechanism or inhibitor is evaluated in more than one cell line, we performed all experiments except for conformation assays in PDXs and multiple PDAC cell lines. While the major focus of this study is paclitaxel resistance, it is of interest to evaluate the role of iHUBs in other first line therapies such in FOLFORINOX and Cisplatin. This will assess if iHUBs activation is induced by certain chemotherapeutic agents or is a general induction effect.

References

- 1 Hamdan, F. H. & Johnsen, S. A. DeltaNp63-dependent super enhancers define molecular identity in pancreatic cancer by an interconnected transcription factor network. *Proc Natl Acad Sci U S A* **115**, E12343-e12352, doi:10.1073/pnas.1812915116 (2018).
- 2 Kutschat, A. P. *et al.* STIM1 Mediates Calcium-dependent Epigenetic Reprogramming in Pancreatic Cancer. *Cancer Res*, doi:10.1158/0008-5472.Can-20-2874 (2021).
- 3 Gryder, B. E., Khan, J. & Stanton, B. Z. Measurement of differential chromatin interactions with absolute quantification of architecture (AQuA-HiChIP). *Nat Protoc* **15**, 1209-1236, doi:10.1038/s41596-019-0285-9 (2020).
- 4 Mumbach, M. R. *et al.* HiChIP: efficient and sensitive analysis of protein-directed genome architecture. *Nature Methods* **13**, 919-922, doi:10.1038/nmeth.3999 (2016).
- 5 Wang, X. *et al.* Bromodomain protein BRDT directs Δ Np63 function and super-enhancer activity in a subset of esophageal squamous cell carcinomas. *Cell Death Differ*, doi:10.1038/s41418-021-00751-w (2021).
- 6 Chu, T. *et al.* Chromatin run-on and sequencing maps the transcriptional regulatory landscape of glioblastoma multiforme. *Nature Genetics* **50**, 1553-1564, doi:10.1038/s41588-018-0244-3 (2018).
- 7 Corces, M. R. *et al.* An improved ATAC-seq protocol reduces background and enables interrogation of frozen tissues. *Nature Methods* **14**, 959-962, doi:10.1038/nmeth.4396 (2017).
- 8 Krijger, P. H. L., Geeven, G., Bianchi, V., Hilvering, C. R. E. & de Laat, W. 4C-seq from beginning to end: A detailed protocol for sample preparation and data analysis. *Methods* **170**, 17-32, doi:<https://doi.org/10.1016/j.ymeth.2019.07.014> (2020).
- 9 Concordet, J.-P. & Haeussler, M. CRISPOR: intuitive guide selection for CRISPR/Cas9 genome editing experiments and screens. *Nucleic Acids Research* **46**, W242-W245, doi:10.1093/nar/gky354 (2018).
- 10 Li, H. & Durbin, R. Fast and accurate short read alignment with Burrows–Wheeler transform. *Bioinformatics* **25**, 1754-1760, doi:10.1093/bioinformatics/btp324 (2009).
- 11 Ramírez, F. *et al.* deepTools2: a next generation web server for deep-sequencing data analysis. *Nucleic Acids Research* **44**, W160-W165, doi:10.1093/nar/gkw257 (2016).
- 12 Dobin, A. *et al.* STAR: ultrafast universal RNA-seq aligner. *Bioinformatics* **29**, 15-21, doi:10.1093/bioinformatics/bts635 (2013).
- 13 Anders, S., Pyl, P. T. & Huber, W. HTSeq—a Python framework to work with high-throughput sequencing data. *Bioinformatics* **31**, 166-169, doi:10.1093/bioinformatics/btu638 (2015).
- 14 Love, M. I., Huber, W. & Anders, S. Moderated estimation of fold change and dispersion for RNA-seq data with DESeq2. *Genome Biology* **15**, 550, doi:10.1186/s13059-014-0550-8 (2014).
- 15 Subramanian, A. *et al.* Gene set enrichment analysis: A knowledge-based approach for interpreting genome-wide expression profiles. *Proceedings of the National Academy of Sciences* **102**, 15545-15550, doi:doi:10.1073/pnas.0506580102 (2005).
- 16 Martin, M. Cutadapt removes adapter sequences from high-throughput sequencing reads. *2011* **17**, 3, doi:10.14806/ej.17.1.200 (2011).
- 17 Langmead, B. & Salzberg, S. L. Fast gapped-read alignment with Bowtie 2. *Nature methods* **9**, 357-359, doi:10.1038/nmeth.1923 (2012).
- 18 Feng, J., Liu, T., Qin, B., Zhang, Y. & Liu, X. S. Identifying ChIP-seq enrichment using MACS. *Nature protocols* **7**, 1728-1740, doi:10.1038/nprot.2012.101 (2012).
- 19 Robinson, J. T. *et al.* Integrative genomics viewer. *Nat Biotechnol* **29**, 24-26, doi:10.1038/nbt.1754 (2011).

- 20 Ross-Innes, C. S. *et al.* Differential oestrogen receptor binding is associated with clinical outcome in breast cancer. *Nature* **481**, 389-393, doi:10.1038/nature10730 (2012).
- 21 Lovén, J. *et al.* Selective inhibition of tumor oncogenes by disruption of super-enhancers. *Cell* **153**, 320-334, doi:10.1016/j.cell.2013.03.036 (2013).
- 22 Whyte, W. A. *et al.* Master transcription factors and mediator establish super-enhancers at key cell identity genes. *Cell* **153**, 307-319, doi:10.1016/j.cell.2013.03.035 (2013).
- 23 Duttke, S. H., Chang, M. W., Heinz, S. & Benner, C. Identification and dynamic quantification of regulatory elements using total RNA. *Genome Res* **29**, 1836-1846, doi:10.1101/gr.253492.119 (2019).
- 24 McLean, C. Y. *et al.* GREAT improves functional interpretation of cis-regulatory regions. *Nat Biotechnol* **28**, 495-501, doi:10.1038/nbt.1630 (2010).
- 25 Talevich, E., Shain, A. H., Botton, T. & Bastian, B. C. CNVkit: Genome-Wide Copy Number Detection and Visualization from Targeted DNA Sequencing. *PLOS Computational Biology* **12**, e1004873, doi:10.1371/journal.pcbi.1004873 (2016).
- 26 Raviram, R. *et al.* 4C-ker: A Method to Reproducibly Identify Genome-Wide Interactions Captured by 4C-Seq Experiments. *PLOS Computational Biology* **12**, e1004780, doi:10.1371/journal.pcbi.1004780 (2016).
- 27 Servant, N. *et al.* HiC-Pro: an optimized and flexible pipeline for Hi-C data processing. *Genome Biology* **16**, 259, doi:10.1186/s13059-015-0831-x (2015).
- 28 Bhattacharyya, S., Chandra, V., Vijayanand, P. & Ay, F. Identification of significant chromatin contacts from HiChIP data by FitHiChIP. *Nature Communications* **10**, 4221, doi:10.1038/s41467-019-11950-y (2019).
- 29 Lieberman-Aiden, E. *et al.* Comprehensive Mapping of Long-Range Interactions Reveals Folding Principles of the Human Genome. *Science* **326**, 289-293, doi:doi:10.1126/science.1181369 (2009).
- 30 Hernandez, M. C. *et al.* Patient-Derived Xenografts Can Be Reliably Generated from Patient Clinical Biopsy Specimens. *J Gastrointest Surg* **23**, 818-824, doi:10.1007/s11605-019-04109-z (2019).
- 31 Hernandez, M. C. *et al.* Successful Secondary Engraftment of Pancreatic Ductal Adenocarcinoma and Cholangiocarcinoma Patient-Derived Xenografts After Previous Failed Primary Engraftment. *Transl Oncol* **12**, 69-75, doi:10.1016/j.tranon.2018.09.008 (2019).
- 32 Leiting, J. L. *et al.* Rituximab Decreases Lymphoproliferative Tumor Formation in Hepatopancreaticobiliary and Gastrointestinal Cancer Patient-Derived Xenografts. *Scientific Reports* **9**, 5901, doi:10.1038/s41598-019-42470-w (2019).
- 33 Kim, M. P. *et al.* Generation of orthotopic and heterotopic human pancreatic cancer xenografts in immunodeficient mice. *Nat Protoc* **4**, 1670-1680, doi:10.1038/nprot.2009.171 (2009).
- 34 Percie du Sert, N. *et al.* Reporting animal research: Explanation and elaboration for the ARRIVE guidelines 2.0. *PLoS Biol* **18**, e3000411, doi:10.1371/journal.pbio.3000411 (2020).

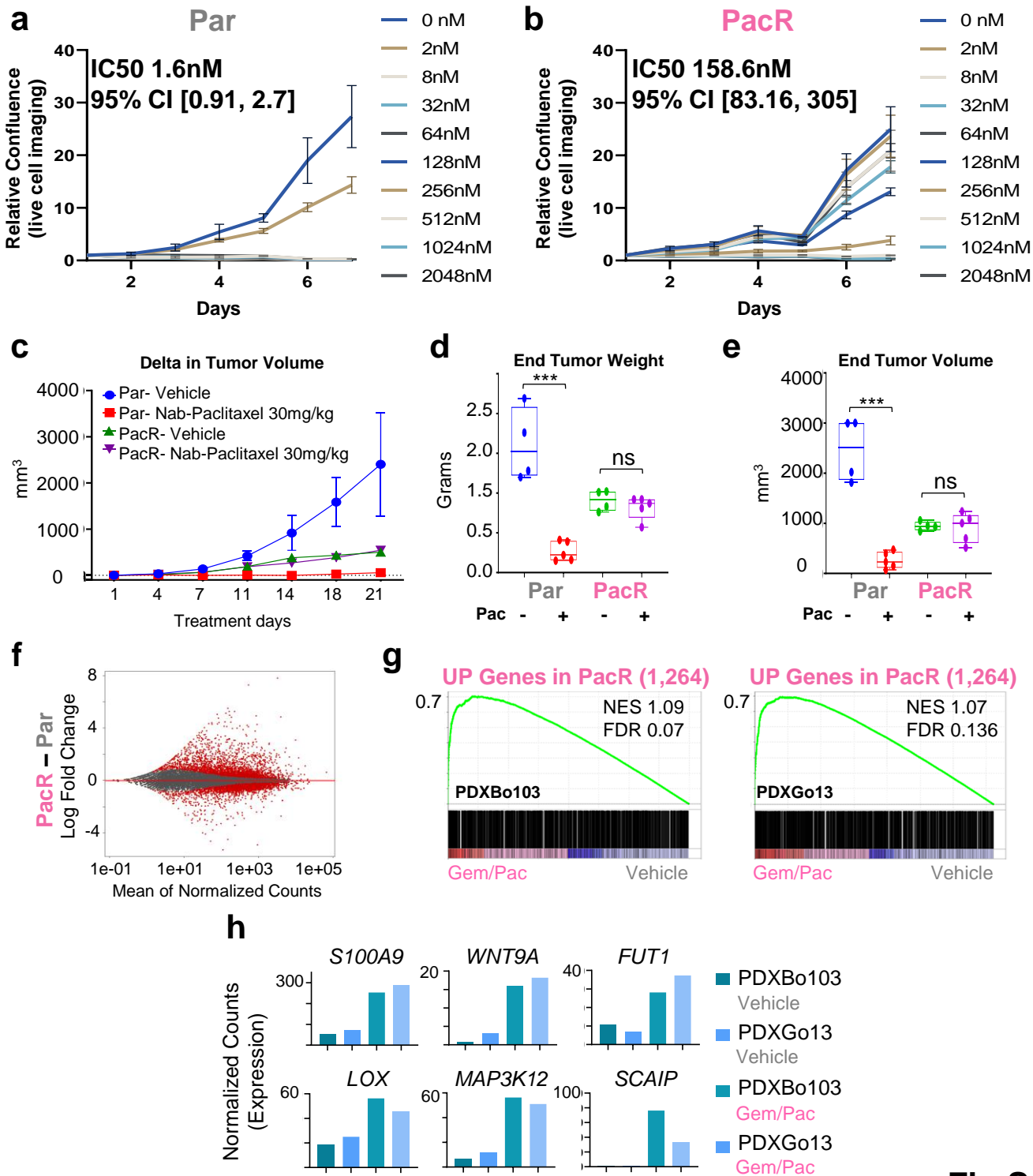


Fig.S1

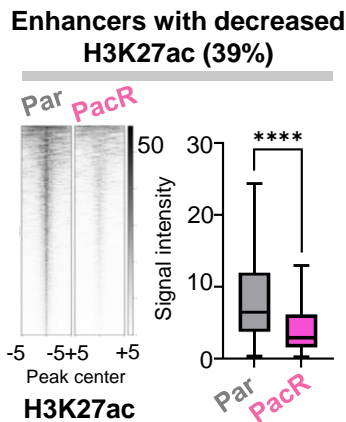
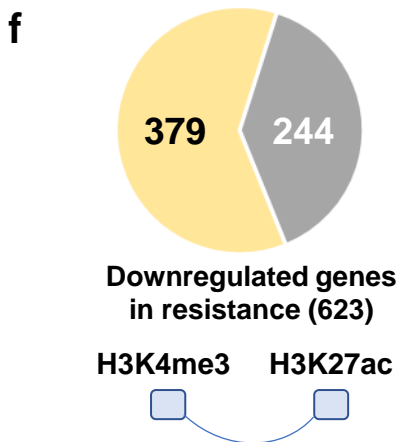
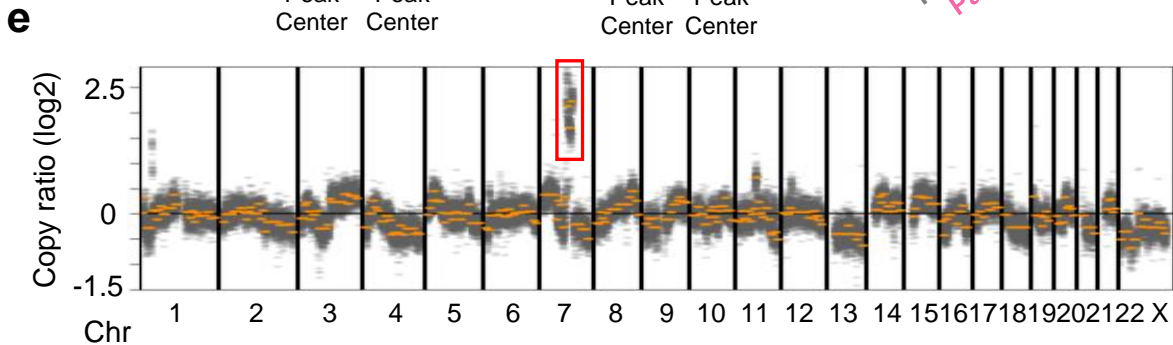
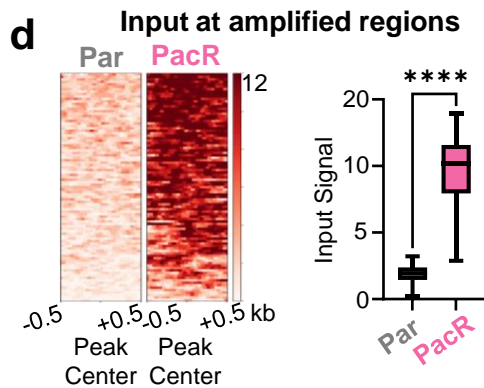
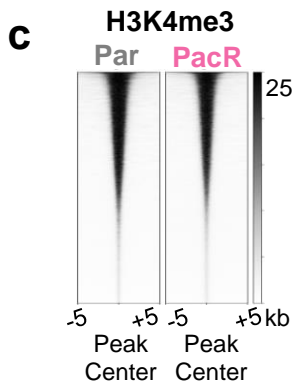
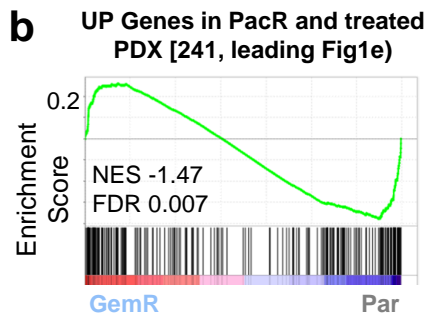
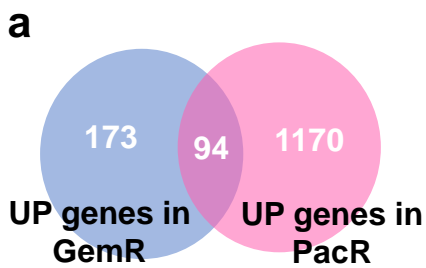


Fig.S2

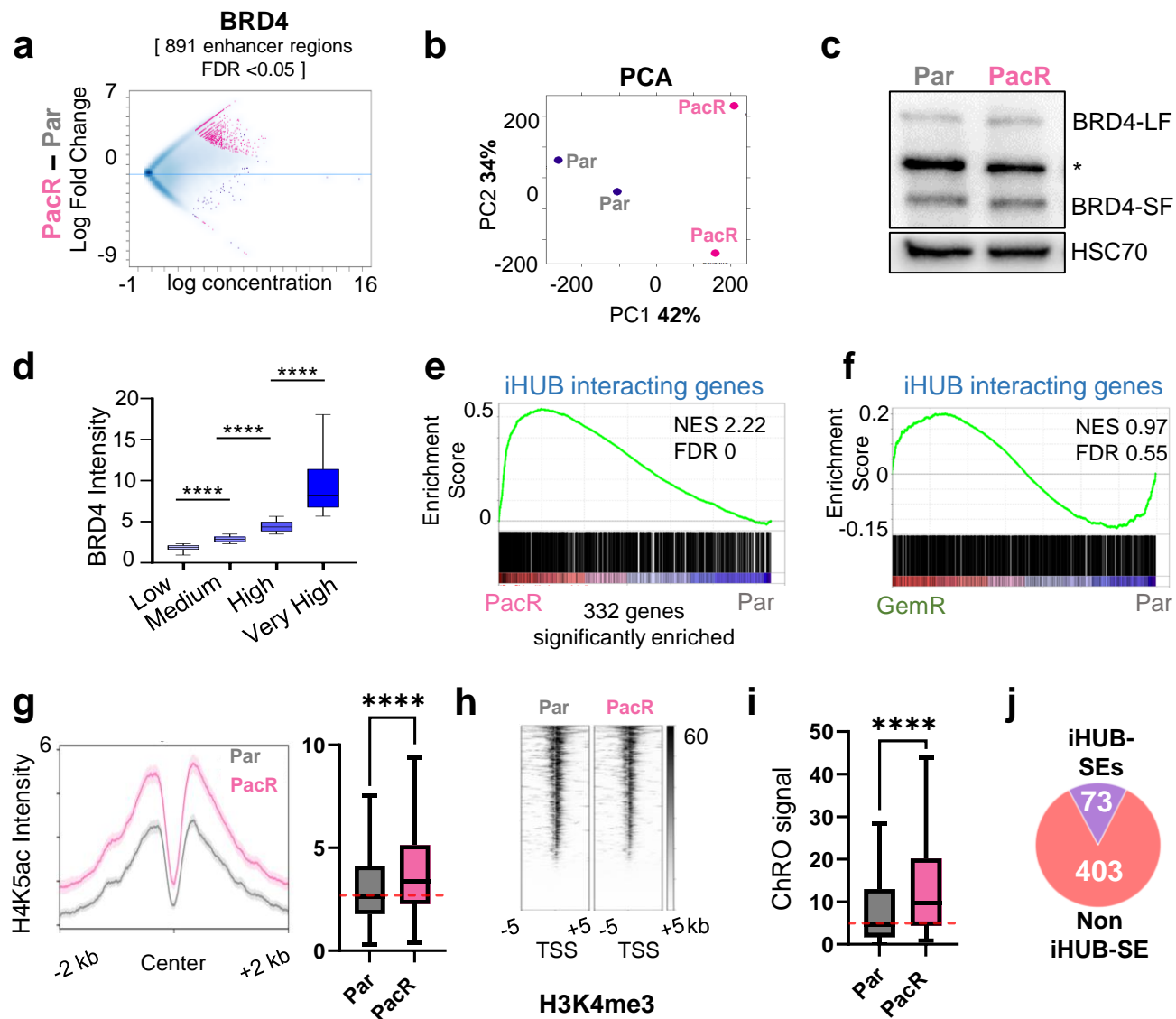


Fig.S3

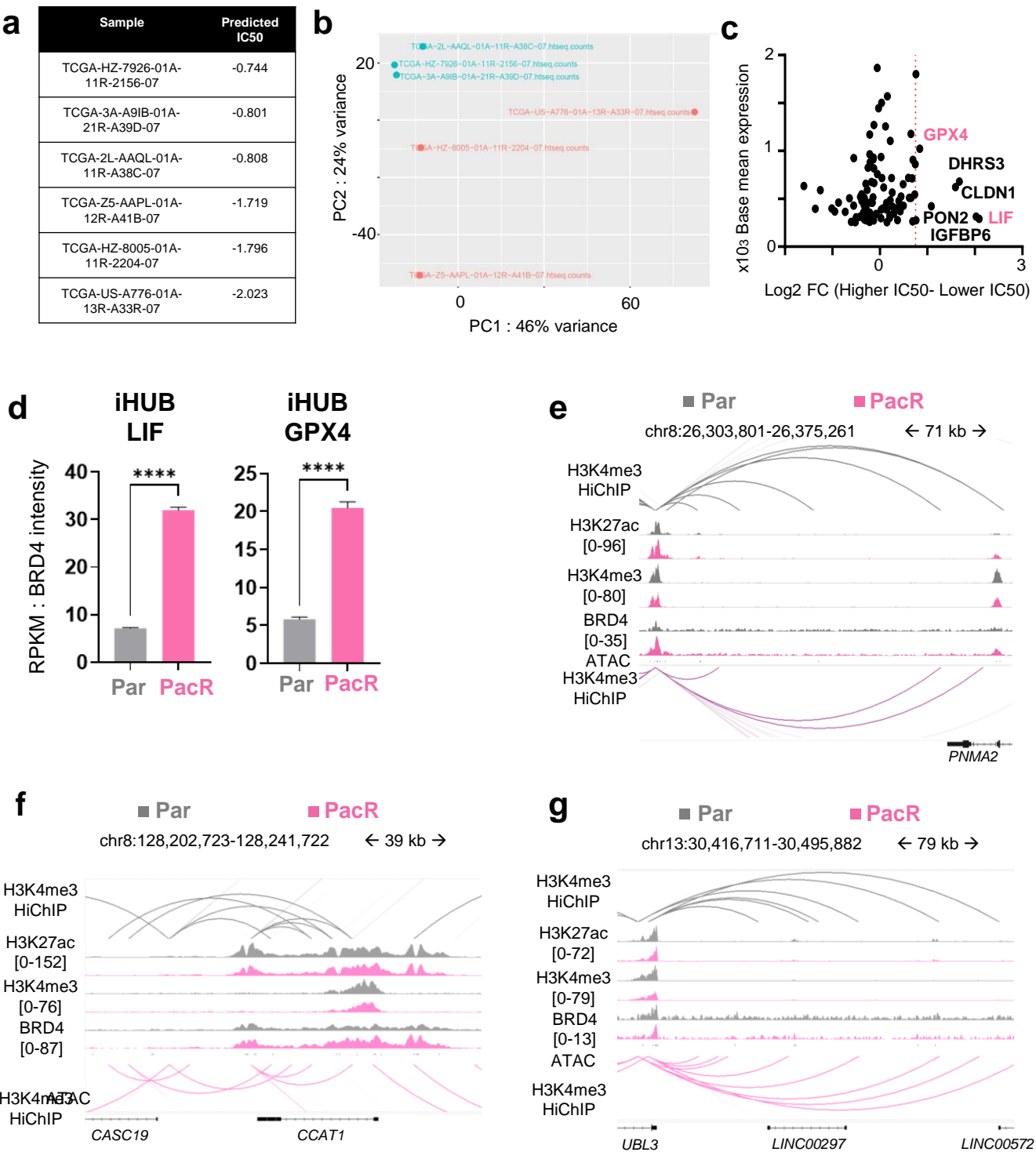
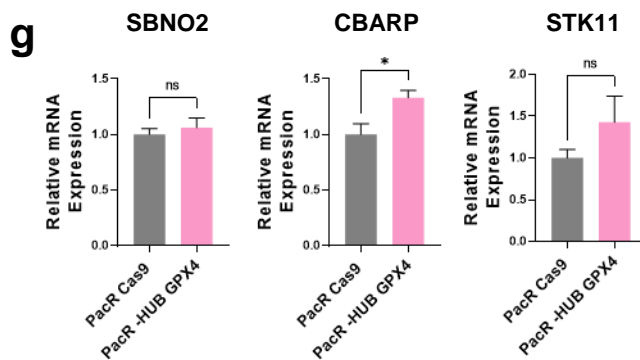
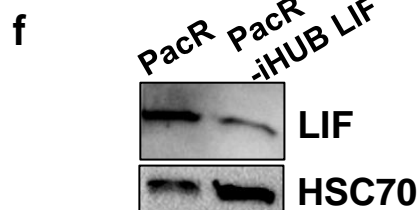
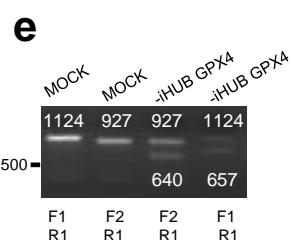
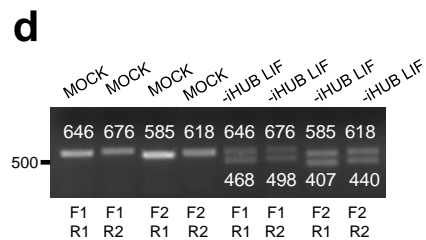
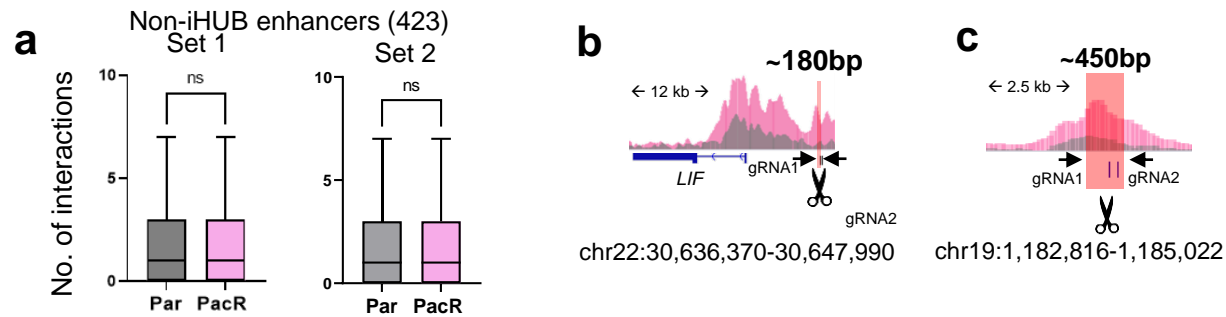
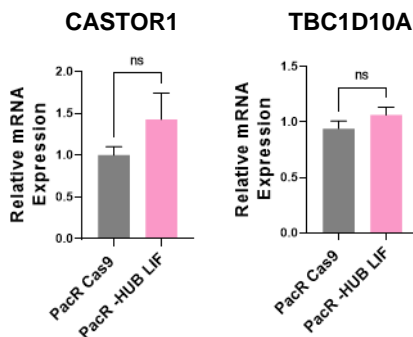


Fig.S4



Genes in the vicinity of GPX4



Genes in the vicinity of GPX4

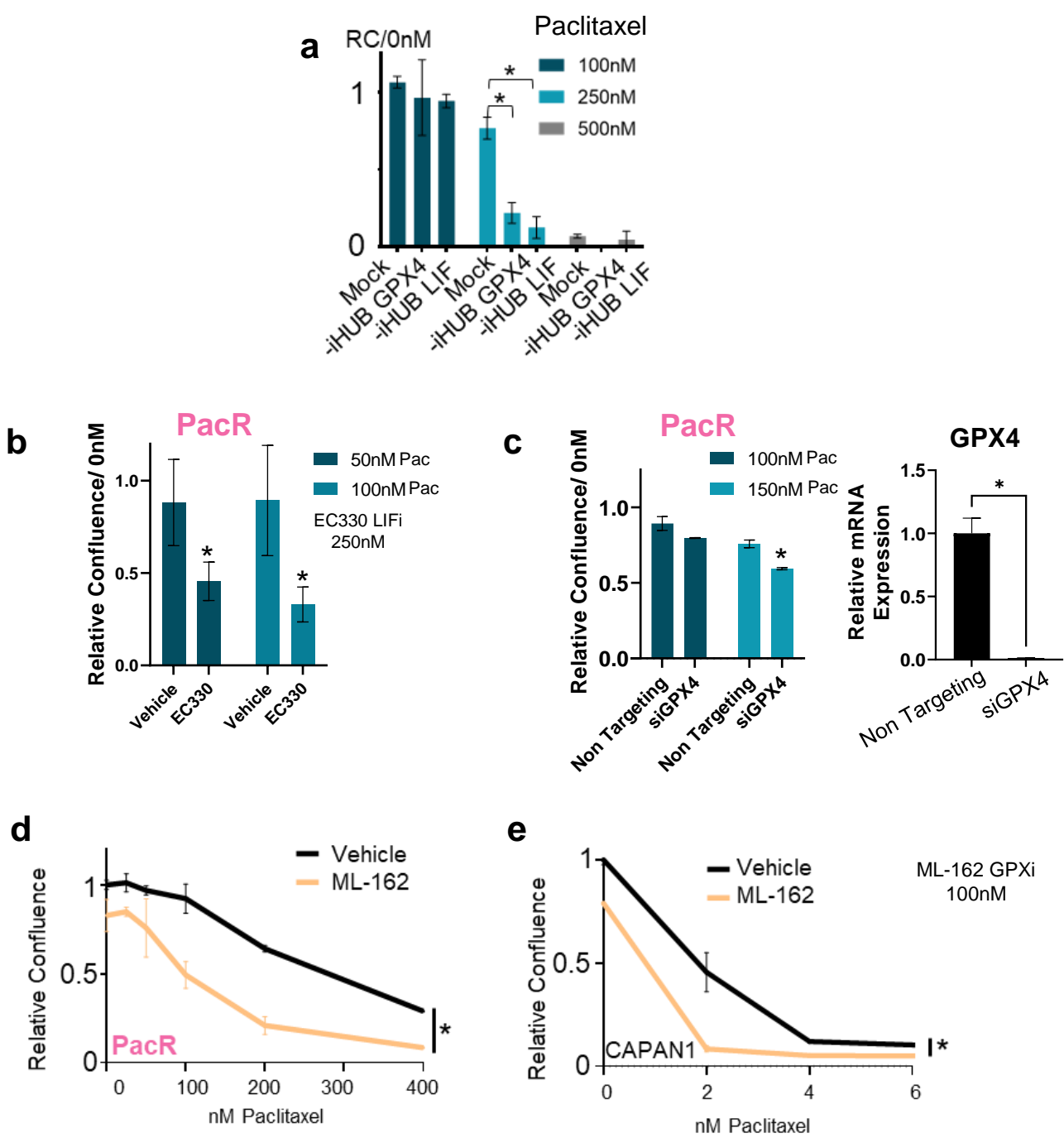


Fig.S6

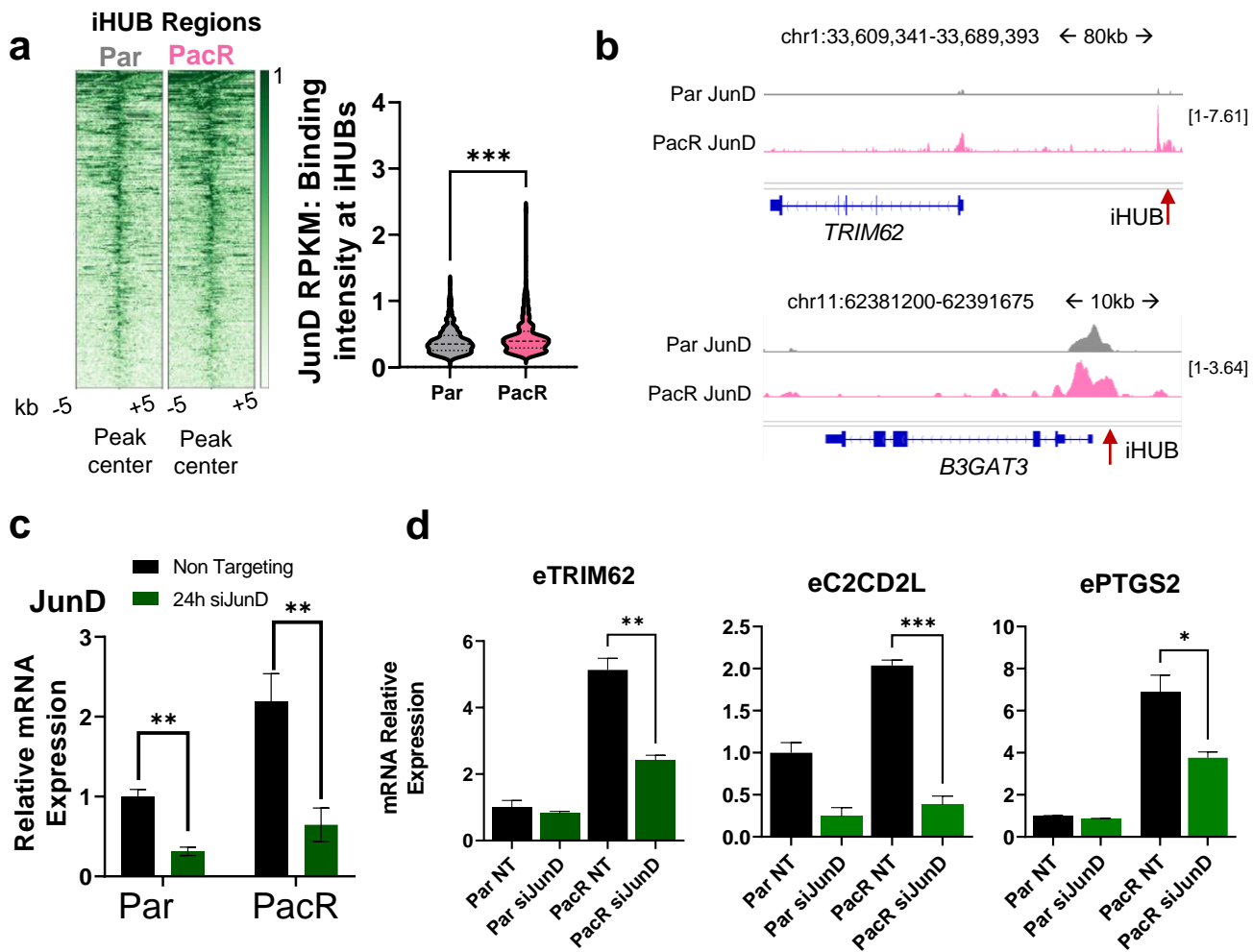
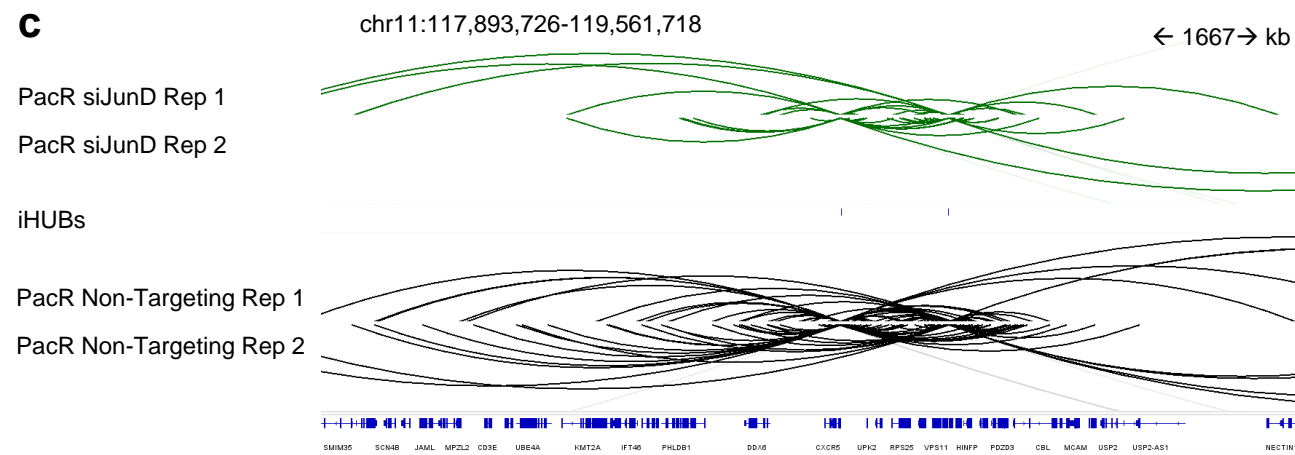
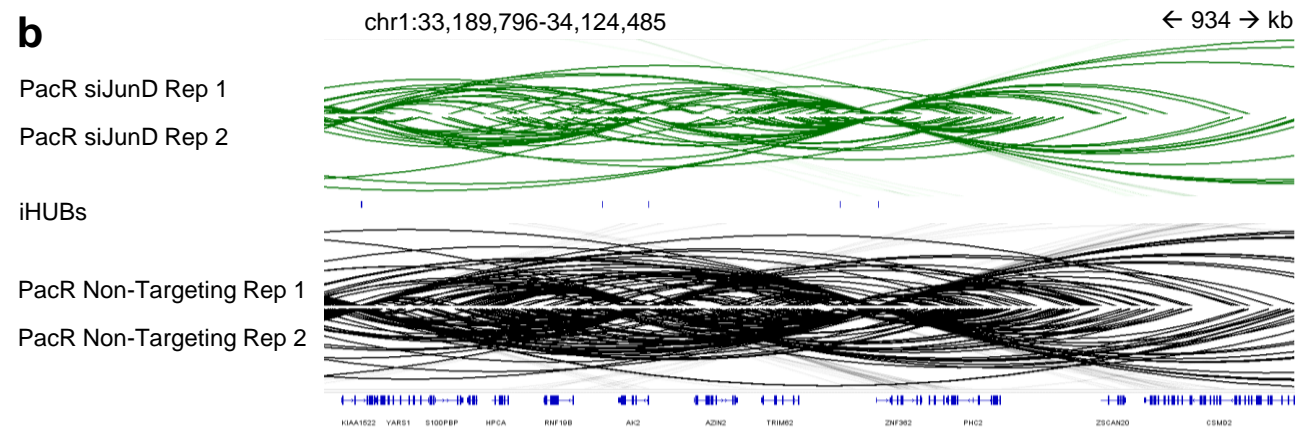
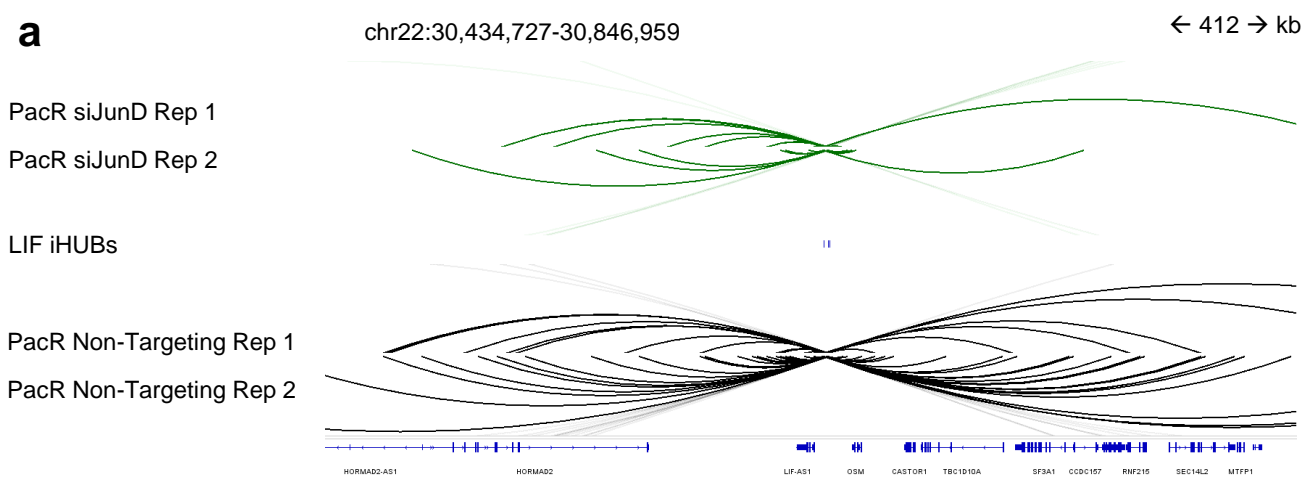


Fig.S7



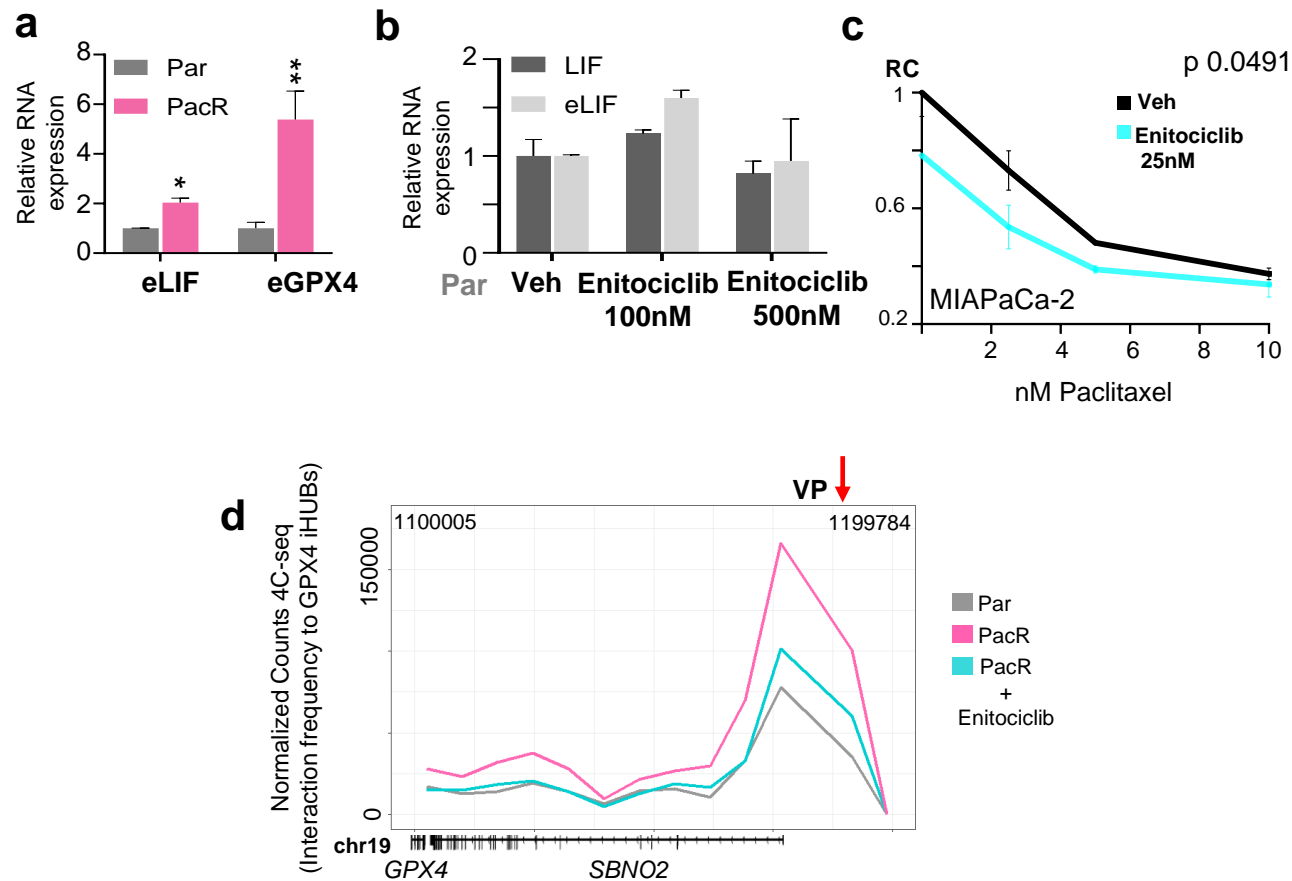
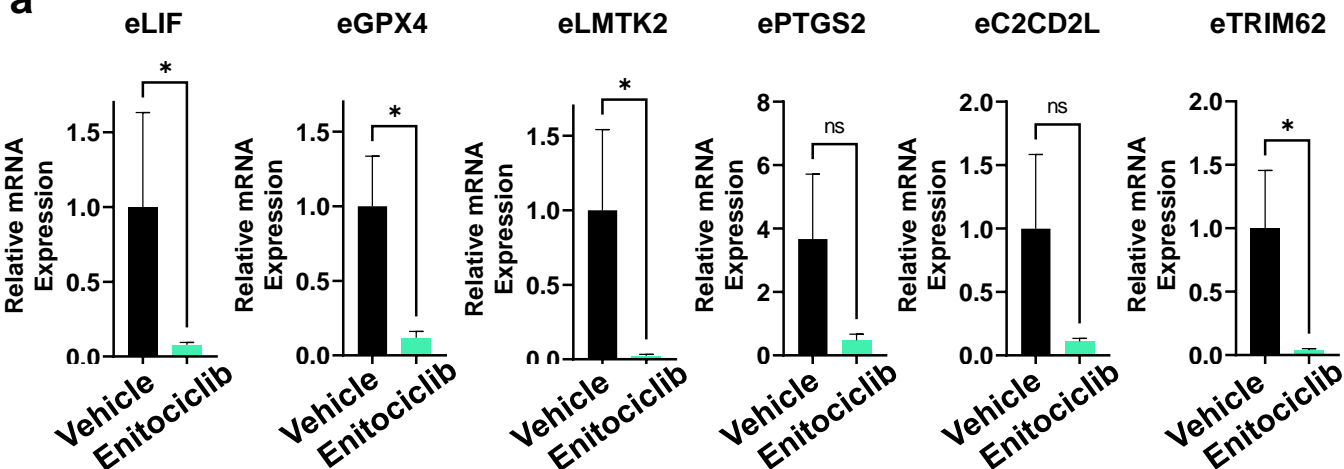


Fig.S9

a**b**

Patient Number	GPX4 Score	LIF Score	Response
10	3+	3+	Poor Response
5	2+	3+	Poor Response
7	2+	2+	Poor Response
2	2+	1+	Partial Response
4	2+	2+	Partial Response
8	2+	2+	Partial Response
9	1+	1+	Good Response
1	2+	1+	Good Response
3	2+	1+	Good Response